# LHCD and Coupling Experiments with an ITER-like PAM launcher on the FTU tokamak

V. Pericoli Ridolfini, M.L. Apicella, E. Barbato, Ph. Bibet[1], P. Buratti, G. Calabrò, A. Cardinali, G. Granucci[2], F. Mirizzi, L. Panaccione, S. Podda, C. Sozzi[2], A.A. Tuccillo

*Associazione EURATOM-ENEA sulla Fusione, Via E. Fermi 45 FRASCATI-Roma, Italy*
*[1]Association Euratom CEA sur la Fusion, CEA Cadarache, St Paul lez Durance, France*
*[2]Associazione EURATOM-ENEA-CNR sulla Fusione, IFP-CNR, Via Cozzi 53 Milano, Italy*

**Abstract.** Successful experimental tests on a PAM (passive active multijunction) prototype antenna for the Lower Hybrid (LH) waves similar to that foreseen for ITER have been carried out on FTU. The power level routinely achieved without any fault in the transmission lines for the maximum time allowed by the LH power plant, i.e. 0.9 s, is 250 kW versus a design value of 270. It corresponds to 50 MW/m$^2$ through the ITER antenna active area if it is scaled for the different LH frequencies (5 GHz in ITER, 8 GHz in FTU) and it is more than 1.4 times the goal of the ITER design (33 MW/m$^2$). The test results validate the main features indicated by the simulation codes, concerning the power handling, the coupling and the launched $N_{||}$ spectrum. The power reflection coefficient $R_c$ is always $\leq 2.5\%$, once the PAM launcher has been properly conditioned, even with the grill mouth retracted 2 mm inside the port shadow, with density in front of the launcher very close or even lower than the cut-off value. The current drive efficiency is comparable to a conventional grill in similar conditions, once the lower directivity is taken into account. The flexibility in the $N_{||}$ spectrum is confirmed by the HXR and ECE spectra. Conditioning the PAM to operate at the ITER equivalent power level has required only one day of RF operation, without a previous baking of the waveguides.

e-mail contact of the main author: pericoli@frascati.enea.it

## 1. Introduction

The possibility of launching lower hybrid (LH) radio-frequency waves into the ITER plasma to control the current radial profile depends on the capability of the launcher to withstand the harsh environment at the plasma border. Since the antennas at present in operation in tokamaks do not satisfy this request, a new concept, called Passive Active Multijunction (PAM) [1] started to be developed jointly by ENEA and CEA (Cadarache, France) EURATOM associations since several years.

The antenna has to satisfy the following fundamental requests. 1) To operate in the full shadow of the vessel port to avoid damage from the large particle flow inside the scrape-off layer (SOL) plasma; 2) to tolerate the heating due to the neutron flux and plasma radiation losses; 3) to preserve a level of power handling and current drive (CD) efficiency acceptable for ITER. These constraints have fixed the minimum power to be coupled through one equatorial port at $P_{LH} \geq 20$ MW, and the CD efficiency ($\eta_{CD}$) at a value larger than, or at least equal to, the best one so far obtained in the world, i.e. $\eta_{CD} \geq 0.3 \cdot 10^{20}$ m$^{-2}$ A/W.

These points imply solving the problem of good power coupling to the main plasma in conditions of almost vanishing plasma in front of the grill together with maintaining CD performances similar to a usual multijunction (MJ). The innovative proposal was to locate cooling ducts in between the LH fed waveguides in the final part of the launcher, except at the front end, where passive waveguides interposed between the active ones restore the usual MJ periodicity [1]. In this way the $N_{||}$ spectrum ($N_{||}$ is the parallel index of refraction), and hence the CD efficiency, can be compared to a standard MJ, provided a strong cross coupling exists between the active and passive waveguides. This in turn occurs if the plasma density in front of the grill is close to the cut-off value or if a thin vacuum layer is present. In this way the

very low density plasma existing in the shadow of the port favours rather than inhibits a good power coupling, as instead it does either for a MJ or for a conventional grill.

The validation of the PAM concept necessitates obviously appropriate experimental tests that have been carried out successfully on FTU, and are described in the present work. The general layout of the FTU PAM and the main technical solutions adopted are described in a recent paper [2]. The main reasons to prefer FTU for the first experimental check were that it could be completed in a rather short time at moderate cost. Indeed, the existing LHCD system required only minor changes, the machine is compact, (major radius R=0.935 m, minor radius a=0.3 m), and the LH pulse length is short (max 1 s), so that even at very high LH power density (close to 100 $MW/m^2$) no cooling is needed and standard materials can be employed. In addition, the presence of other independent conventional grills that can be phased to give $N_{||}$ spectra very similar to those calculated for the PAM, could allow a direct comparison with the well-assessed performances of common launchers.

## 2. Experiment

The experimental results on the PAM performances in FTU, scaled to the ITER dimensions and parameters, have supported the main expectations for using such a launcher in ITER.

The LH power coupled through the PAM for the maximum LH pulse length allowed by the power system, i.e. ≈0.9 s, has been 245 kW. Almost steady conditions are maintained and no fault in the transmission lines or in the grill mouth occurs. The power density on the active area of the grill is 73 $MW/m^2$, close to the design value of 80 $MW/m^2$ (270 kW total). This is 1.4 times higher than the value of 52 $MW/m^2$ (175 kW total) that corresponds to the target of 33 $MW/m^2$ for the ITER launcher (20 MW total), when the different LH frequencies, 8 GHz in FTU, 5 GHz in ITER, are taken into account [3].

The PAM could operate routinely at 250 kW level with no previous vacuum baking, after a simple conditioning procedure for two days, necessary to exhaust the gas adsorbed onto the internal surfaces. The waveguides are fed during the plasma discharges by ON/OFF modulated LH power with an average total ‘ON’ time of about 0.5-0.6 s over a total permitted LH time length of 0.9 s. About 30 discharges, are sufficient to reach the ITER equivalent power level of 170 kW.

No additional pumping has been installed, because the poor conductance of the waveguides would make it scarcely useful on the time scale of the FTU pulse duration, even for large outgassing [4]. No degrading of the cleanliness of the waveguides is observed over one month. This procedure, however, maintains a sort of local character, being fully effective only for the region where the electron multipactoring is higher. Indeed, it had to be repeated after changing either the antenna position respect to the vessel by more than 5 mm, or the pattern of the total magnetic field that occurs when the plasma current $I_p$ or the toroidal magnetic field $B_T$ are varied. Baking the wave-guides should minimize this disadvantage, since it cleans thoroughly their surface.

A well conditioned antenna could couple to the plasma even higher power: the design value of 270 kW is achieved with a 0.2/0.08 s ON/OFF cycle on 1.0 s total duration, and more than 300 kW (89 $MW/m^2$) on a single pulse 0.07 s long, terminated by strong outgassing inside a waveguide. Only the lack of time impeded to try longer times in both cases.

Very good coupling is always achieved after a proper conditioning that makes negligible the outgassing from the waveguide walls caused by the LH electric field. The average power reflection coefficient $R_c$ stays below 2.5%, even with the grill mouth retracted 2 mm inside the port shadow, with density in front of the launcher ($n_{e,PAM}$) very close to the cut-off value ($n_{e,c.o.}=0.79\cdot10^{18}$ m$^{-3}$).

In Fig. 1 the experimental $R_c$ values are plotted versus $n_{e,PAM}$, taken as an average from the measurements of 4 Langmuir probes located aside the grill (O symbols), together with the prediction from SWAN-2D [5] and GRILL-3D [6] codes calculations, shown as lines. The discrepancies are within the errors associated with Langmuir probe measurements. The $R_c$ increase closer to the cut-off density is predicted instead only by GRILL-3D. Its minimum despite is quite low (≈1.2%), never reaches the level ≤0.5% predicted by the codes. The failure to attain the $R_c$ minimum is found with the FTU conventional grill too, [7] and it is observed also in other tokamaks. Finer comparisons, as to consider $R_c$ for different $N_{||}$ spectra or its pattern along one grill row, are difficult because of the accuracy of the measuremnts and of the strongly varying density in front of the antenna. This is mainly caused by the uneven length of the field lines in the scrape-off plasma (SOL) [8], which is particularly developed close to the wall because of the field distortion by the magnetic ripple.

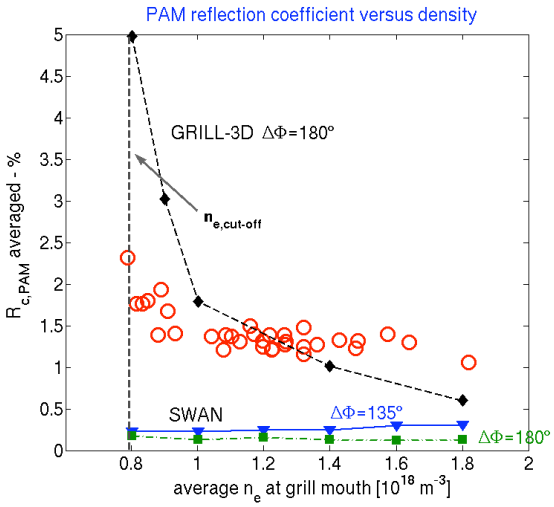


*Fig. 1 – Average power reflection coefficient of the PAM versus the average density at the grill mouth, according to Langmuir probes mounted aside the grill. Code calculations, shown as lines, are plotted for SWAN and GRILL-3D codes*

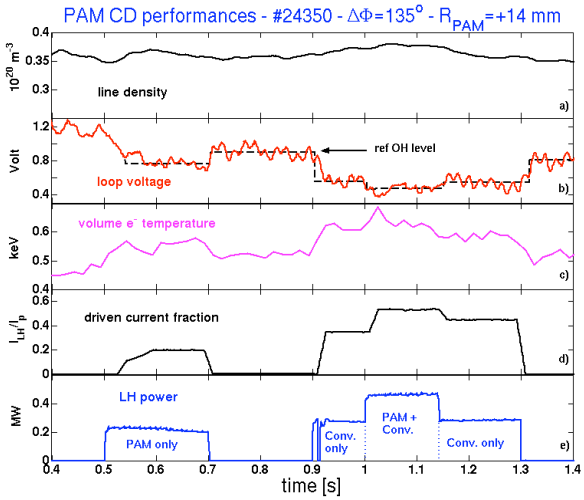


*Fig. 2 – Current drive effects. Comparison between PAM and a conventional grill. Time traces of: a) line averaged density, b) loop voltage, c) volume averaged electron temperature, d) ratio of the LH driven to the total plasma current, e) coupled LH power*

The performance of the PAM antenna in terms of the CD efficiency is shown in Fig. 2, where the most relevant macroscopic quantities are plotted versus time for a discharge where the PAM and a conventional grill taken as reference are excited either alone or together. The first phase to be considered is that when the PAM only is excited, the second is a reference ohmic segment, the third a LH pulse from the conventional grill alone, named G4, followed then by a superimposition of the PAM power onto the G4 grill.

The conventional grill is set to launch a $N_{||}$ spectrum similar to the PAM: the peak value is the same, $N_{||,pk}$≈2.24, but the directivity, i.e. the fraction of the total power launched in the CD direction, is larger, 80% against 65%. The magnitude of the LH driven current is deduced as in Ref. [9] from the evaluation of the residual ohmic current, considering the drop of the loop

voltage $V_l$ and the resistivity change due to the variation of the impurity content ($Z_{eff}$) and of the electron temperature respect to the ohmic phase, namely from:

$$\frac{I_{LH}}{I_p} = 1 - \frac{V_{l,LH}}{V_{l,OH}} \cdot \frac{\left\langle T_{e,LH}^{3/2} \right\rangle}{\left\langle T_{e,OH}^{3/2} \right\rangle} \cdot \frac{Z_{eff,OH}}{Z_{eff,LH}} \quad (1)$$

The residual ohmic current fraction is the second term in the r. h. s. The larger driven current fraction for G4, visible in the figure, is due to the higher directivity and coupled power, and to the higher electron temperature, which is well known to enhance $\eta_{CD}$ in FTU [9]. Within the limits of the experimental errors the effect of the two grills are also additive.

On the basis of many shots the CD properties of the PAM are illustrated in Fig. 3, where the $I_{LH}/I_p$ is plotted versus the parameter $h=P_{LH}/(\bar{n}_e \cdot I_p \cdot R) \cdot 6/(Z_{eff}+5)$; $P_{LH}$ is the total LH coupled power, $\bar{n}_e$ is the line averaged plasma density and R=0.935 m is the FTU major radius, as in Ref. [9]. This quantity is chosen as it holds the simple relation $I_{LH}/I_p=h \cdot \eta_{CD}(Z_{eff}=1)$, directly derived from the definition $\eta_{CD}(Z_{eff}=1)=I_{LH}\bar{n}_e \cdot R/P_{LH} \cdot (Z_{eff}+5)/6$. All the data points have fixed $B_T$ to 7.1 T and $I_p$ to 0.35 MA, while $\bar{n}_e$ ranges in $0.3\text{-}0.55 \cdot 10^{20}$ $m^{-3}$. Evaluations have been made for the phases with PAM alone, with G4 alone, with the combination of two, and also for the incremental effect of the PAM on the G4 only phase, denoted by different symbols. Within the experimental errors the various situations cannot be distinguished: the PAM and conventional grill CD capability are well aligned and their contribution is additive to that of other grills, as for normal operations. The apparent deviation from the FTU usual linearity of similar plots [9] is reduced, but persists, if the waves directivity, neglected for these data points, is taken into account. This is a consequence of the non negligible ohmic conductivity of the fast electron tail in cases of quite low collisionality, i.e. low density as pointed out in Ref. [9], when the LH power is not enough to drive more than 40% of the total current and to depress sufficiently the residual ohmic electric field, as for the discharge shown in Fig. 2.

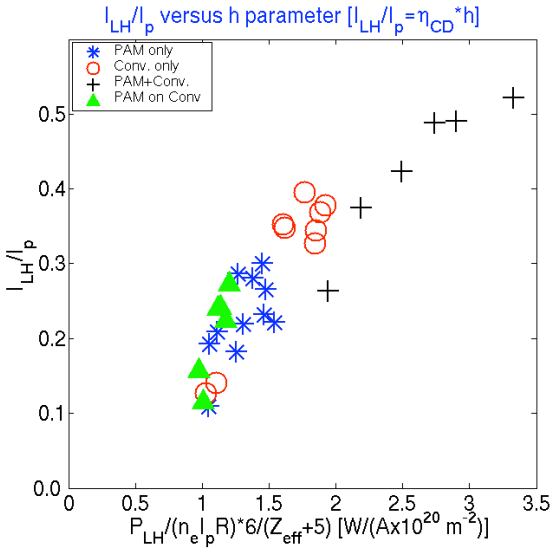


*Fig. 3 – Fraction of the LH driven current versus the quantity h defined in the text. $B_T$=7.1 T, $I_p$=0.35 MA, $\bar{n}_e$=3.2-5.5·10^19 m^-3. Triangles describe the incremental effect of the PAM on the conventional grill alone phase*

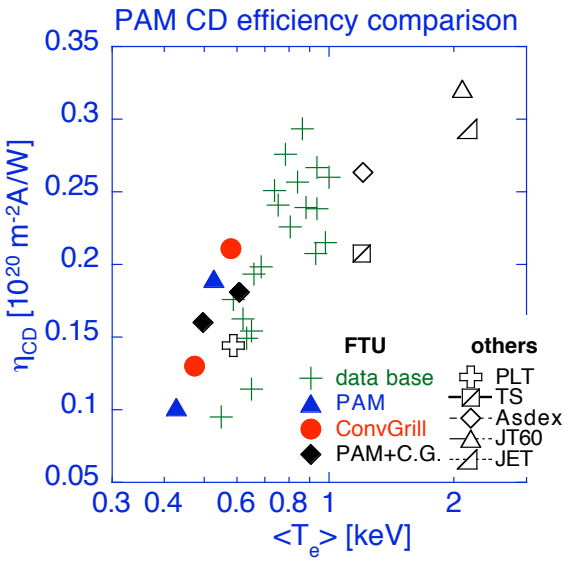


*Fig. 4 – CD efficiency versus $<T_e>$ of the PAM (full symbols) compared with the FTU data base (crosses) and other tokamaks' efficiencies [10] (empty symbols)*

To compare the CD efficiency with the FTU data base, which is published in Ref. [10] where also other tokamaks are considered, $\eta_{CD}$ has been estimated for a couple of $<T_e>$ (volume averaged electron temperature) values where preferentially gather the points for each of the three configurations, PAM only, G4 only and PAM+G4. An average among these various points is assumed. A slight overestimate of the ratio $I_{LH}/I_p$ is however possible, as pointed out just above. The results are illustrated in Fig. 4. As expected, the PAM $\eta_{CD}$ points follow the same increasing trend with $<T_e>$ as the rest of the FTU data base and are located in the bottom part ($\eta_{CD} \leq 0.21 \cdot 10^{20}$ $m^{-2}A/W$) due to the low values of $<T_e>$, which is $\leq 0.55$ keV. The usual range of FTU operation is $<T_e> \geq 0.8$ keV where $\eta_{CD} \approx 0.25 \cdot 10^{20}$ $m^{-2}A/W$.

The specific behavior of the LH generated fast electron tail has been analyzed by means of a fast electron bremsstrahlung (FEB) camera and of a microwave Michelson interferometer. The FEB camera, recently installed, detects the HXR (hard X-rays) photons in the energy range 20-140 keV with 20 keV spectral resolution emitted perpendicularly to $B_T$, whereas the interferometer analyses spectrally the electron cyclotron emission (ECE) in the 100-450 GHz frequency interval approximately. The ECE signal from suprathermal electrons is easily distinguished from the rest of the spectrum due to the relativistic frequency down shift.

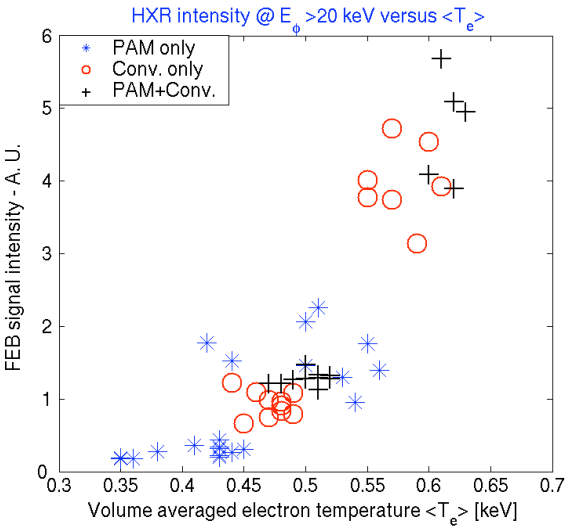


*Fig. 5 – Perpendicular hard X- ray emission ($E_\varphi$ =20- 140 keV) versus the volume averaged electron temperature, for the different combination of the LH grills. PAM only: *, Conv. Grill only: O, PAM+C.G.: +*

Figure 5 shows the plot of the HXR intensity collected along the central viewing chord as a function of $<T_e>$ for the three different combinations of the two operating LH grills. The same symbols as in Fig. 3 are used. As for the CD efficiency, $<T_e>$ is the macroscopic plasma quantity that best orders the data. This occurs also for the ECE intensity in almost the entire down shifted range. Then the electron temperature is the plasma quantity that first governs the formation of the fast electron tail. Again no distinction can be made between the PAM and the conventional grill either if they are used alone or together.

The PAM flexibility in the $N_{||}$ spectrum also has been studied from the behavior of the suprathermal $e^-$ tail. Significant relevant information are indeed hard to derive from the macroscopic plasma parameters, as the loop voltage, because the low available power causes only small changes. In addition, the FTU PAM design is not optimized for large variation of the $N_{||}$ spectrum: when we vary the phase shift between adjacent multijunctions from the optimum value $\Delta\Phi$=135° to $\Delta\Phi$=0°, $N_{||,pk}$ does decrease from ≈2.24 to ≈1.7, but the waves directivity drops from 65% to 53% approximately, almost balancing the gain on the driven current expected from having extended the tail to higher velocities. However ECE and FEB measurements provide a mean to see such an extension, as shown by figures 6 and 7.

The HXR signals, detected along the central chord in distinct energy windows, are compared in Fig. 6 for two discharges with same density, $\bar{n}_e \approx 0.53 \cdot 10^{20}$ $m^{-3}$, but different spectra, $N_{||,pk} \approx 1.7$ and ≈2.4 ($\Delta\Phi$=180°). In both phases, with PAM alone (top) and PAM+G4 (bottom), the faster spectrum does create a faster tail. The effect is of course larger when only the PAM

is excited. The two spectra start do differ for $E_\varphi$>90 keV, just for energy ranges of electrons traveling faster than a LH wave with $N_{||}$≈1.9 (relativistic γ=1.165). The unchanged loop voltage in the two discharges ensures that the distinction between the two spectra is not guided by the residual electric field. This is lower than the Dreicer threshold for a free acceleration of an electron with the same velocity as a LH wave with $N_{||}$=1.7, which in FTU is 2.6 V. The constant $V_{loop}$ is also consistent with a balance between the variation of the CD efficiency and of the directivity, when changing $N_{||,pk}$, as anticipated above.

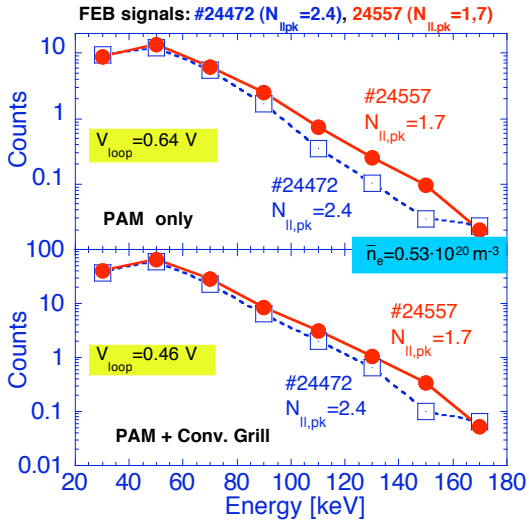


*Fig. 6 – FEB signals detected along the central chord. Two different phasing of the PAM are compared for the PAM only and PAM+ conventional grill phases. $B_T$=7.1 T, $I_p$=0.35 MA*

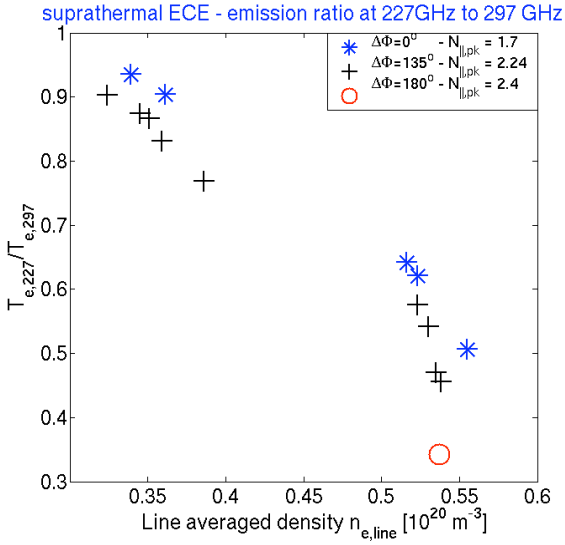


*Fig. 7 – Ratio of the ECE signals at the two downshifted frequencies 227 and 297 GHz versus line density for three different PAM $N_{||}$ spectra. The faster spectrum has always the larger ratio*

Figure 7 shows instead the ratio of the ECE signals at 227 GHz on that at 297 GHz for the three spectra of the PAM tested. These two frequencies are the most apart ones available in the downshifted range that still do no overlap to other thermal EC harmonics. In this frequency range the plasma is optically thin and the collected radiation is proportional to the number of emitting electrons, hence the intensity ratio is a measure of the ratio of the relevant electron population. Despite the optical thinness does not allow spatial resolution, the frequency separation is large enough for the radiation to come mostly from distinct and separate parts of the electron tail, provided the LH deposition is bounded within half the minor radius. This latter condition has been verified through the FEB radial profiles and the calculation of the fast ray-tracing code (FRTC [11]), with the $N_{||}$ spectrum given by the grill code. Ref. [12] shows that the consistency between FEB and FRTC is particularly satisfactory for $\bar{n}_e > 0.4\cdot10^{20}$ m$^{-3}$ where the radial diffusion of the fast electrons can be neglected. For electrons located on the equator, half way between the torus major radius and the outer walls, the radiation at 297 and 227 GHz is associated to γ=1.09 and γ=1.43 respectively, corresponding to LH wave parallel velocities of $N_{||}$=2.5 and 1.4. Figure 7 shows that we can actually change the PAM $N_{||}$: indeed all over the density range the (calculated) faster spectrum does produce a faster electron population.

To check whether the measured HXR spectrum were consistent with the distortion of the electron distribution function caused by the LH waves, we calculated the perpendicular bremsstrahlung emission along the FEB viewing chords. The temperature and density radial profiles are measured and the current profiles are calculated by the equilibrium reconstruction

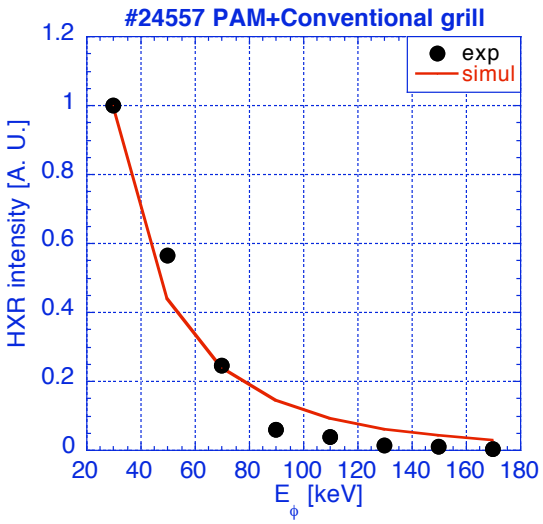


*Fig. 8 – Measured and simulated hard X-ray spectra along the central chord of the FEB. The values are normalized to their maximum value to get free from geometrical factors*

code from magnetic measurements. Instead, suppositions must be made for the $e^-$ fast tail. This is assumed to extend in the velocity space from about $w_1=3.5\cdot v_{th,e}$ to $w_2=c/N_{||,pk}$ (c=light speed, $v_{th,e}$=electron thermal velocity) and to contain a fraction of electrons that accounts for the driven current. This fraction is $n_{e,tail}/n_{e,bulk}=0.001$ for the case here considered and shown in Fig. 8. Here the experimental and computed spectra along the central chord are plotted. The values are normalized to their maximum value to get rid of geometrical factors. The combined PAM+G4 phase, shown as an example, is chosen to diminish the statistical error on the FEB counts; however also for the PAM alone the agreement between code and experiment is satisfactory enough.

Other important PAM features, as the effect of the edge density on the spectrum directivity are beyond the accuracy of our measurements, due to the low available power and the limited spectrum directivity.

## 3. - Conclusions

The tests carried out at FTU on a prototype PAM antenna, proposed as LH wave launcher for ITER in order to overcome the heavy environment, have validated this innovative launcher concept on the physics side and also for some technical aspects.

Very good coupling is obtained throughout the SOL plasma, provided the antenna is properly conditioned to avoid gas release from the waveguide walls. On average the reflection coefficient $R_c$ is ≈1.3%, and never exceeds 2.5%, even with almost evanescent plasma in front of the grill, as when this is fully retracted inside the port (up to 3 mm) to simulate the ITER operation and the density at its mouth is equal or even lower than the cut-off value.

The CD efficiency is not degraded respect to a conventional grill launching a similar $N_{||}$ spectrum, taking into account the lower power directivity. This is derived from the change in the macroscopic plasma parameters and from the analysis of the electro-magnetic emission by the LH generated fast $e^-$ tail. This latter is studied in the hard X-ray range (bremsstrahlung radiation) and in the sub-millimeter wave region (relativistically downshifted electron cyclotron emission). The spectra of both these kind of radiation give evidence of the PAM flexibility in the $N_{||}$ spectrum.

From the technical side the power handling capability is well above the minimum required for ITER: instead of 33 MW/m$^2$, a possible target value is 50 MW/m$^2$, according to the usual frequency scaling from 8 GHz in FTU to 5 GHz envisaged for ITER. Conditioning the waveguides, even though essential for using the PAM, does not require lengthy or particular techniques and the waveguide cleanliness persists over long time. Finally no damage has been detected on the PAM mouth after its removal from the FTU port.

All these features give reasonable confidence in using a PAM antenna in ITER, even though other very crucial aspects will be in the near future investigated on Tore Supra tokamak at Cadarache, CEA, France. In particular it will be studied the response to a very prolonged RF excitation, up to 1000 s, which is of the order of the time scale of the particle wall saturation and of the thermalization of the whole device and to large heat loads. Total power flows across the last closed magnetic surface are foreseen to be up to 0.19 $MW/m^2$ for 30 s, or 0.12 $MW/m^2$ for 1000 s [13], to be compared with 0.22 $MW/m^2$ predicted for ITER FEAT.

**Aknowledgements**

The authors wish to thank the technical staff, M. Aquilini, S. Di Giovenale, P. Petrolini for their hard work onto the PAM and the overall LH system.

**References**

[1] BIBET, Ph., LITAUDON, D., MOREAU, D., "Principle of a retroreflecting LH antenna", Proc. of the "IAEA tech. Comittee meeting on RF launchers for plasma heating and current drive", Nov 1993, Naka (Japan)
[2] MIRIZZI, F., et al., "Experiment with the PAM Launcher for FTU" Proc. 20th Symposium on Fusion Engineering (SOFE 2003). 14-7 Oct. 2003, S. Diego (CA - USA), in press.
[3] AQUILINI, M., BALDI, L., BIBET, Ph., BOZZI, R., BRUSCHI, A., et al, Fus. Sci. Tech. **V. 45**, No. 3 (May 2004), Ch. 11, p 459-482
[4] APICELLA, M.L., private communication
[5] LITAUDON, X., MOREAU, D., Nucl Fus., **V. 30**, p. 471 (1990)
[6] IRZAK, M., SHCHERBININ, O: Nucl Fus., **V. 35**, p. 1341 (1995)
[7] TUCCILLO, A.A., et al, '8 GHz Experiment on FTU', Strong Microwaves in Plasmas (Proceedings of the Int. Workshop on Strong Microwaves in Plasmas, Nizhny Novgorod, Russia, August 15-22 1993), **V. 1**, p. 47, (1994)
[8] LEIGHEB, M., PERICOLI RIDOLFINI, V., ZAGÓRSKI, R., J. Nucl. Mat., **V. 241-243**, p. 914, (1997)
[9] PERICOLI RIDOLFINI, V., et al, Phys. Rev. Lett. **V. 82**, No. 1, p. 93 (1999)
[10] PODDA, S., et al, 19th IAEA Conf. on Fusion Energy, Lyon, France, 14-19 Oct. 2002 (IAEA-CN94-PD/P-07).
[11] ESTERKIN, A.R. and PILIYA, A.D., Nucl. Fusion **38**, 1501, (1996)
[12] BARBATO, E., SAVELIEV, A., " Benchmarking of LHCD numerical modelling on FTU discharges and application to ITER-FEAT scenarios " EPS Conference 2004 London, GB , P2.104
[13] EURATOM-CEA Association, "CIMES – 1", Rep. EUR(00) CCE-FU 7/8.9a, Cadarache, France, June 2000